NANO LETTERS

2008
Vol. 8, No. 9
2706-2711

Visualizing the Local Optical Response of Semiconducting Carbon Nanotubes to DNA-Wrapping

Huihong Qian,[†] Paulo T. Araujo,[‡] Carsten Georgi,[†] Tobias Gokus,[†] Nicolai Hartmann,[†] Alexander A. Green,[§] Ado Jorio,[‡] Mark C. Hersam,[§] Lukas Novotny,[||] and Achim Hartschuh*[,†]

Department Chemie and Biochemie and CeNS, Ludwig-Maximilians-Universität München, 81377 München, Germany, Departamento de Física, Universidade Federal de Minas Gerais, Belo Horizonte, MG, 30123-970 Brazil, Department of Materials Science and Engineering and Department of Chemistry, Northwestern University, Evanston, Illinois 60208-3108, and The Institute of Optics, University of Rochester, Rochester, New York 14627

Received April 11, 2008; Revised Manuscript Received June 16, 2008

ABSTRACT

We studied the local optical response of semiconducting single-walled carbon nanotubes to wrapping by DNA segments using high resolution tip-enhanced near-field microscopy. Photoluminescence (PL) near-field images of single nanotubes reveal large DNA-wrapping-induced red shifts of the exciton energy that are two times higher than indicated by spatially averaging confocal microscopy. Near-field PL spectra taken along nanotubes feature two distinct PL bands resulting from DNA-wrapped and unwrapped nanotube segments. The transition between the two energy levels occurs on a length scale smaller than our spatial resolution of about 15 nm.

Semiconducting single-walled carbon nanotubes (SWNTs) as photoluminescent quasi-one-dimensional systems have attracted enormous scientific interest and have large potential for various applications in photonics and opto- and nanoelectronics.[1−3] Photoluminescence (PL) of nanotubes results from exciton recombination and occurs in the near-infrared spectral range with emission energies controlled mainly by the nanotube structure (n,m).[4−8] Since nanotubes consist of surface atoms only, the detected emission energy is very sensitive to the nanotube environment, making them promising candidates for sensing applications.[9] At present, the influence of the environment is described by its relative dielectric constant ε influencing exciton binding energies but also renormalizing the band gap through charge carrier screening.[10−14] As a result, the emission energy of nanotubes is modulated by the dielectric constant, which can be expected to be nonuniform along nanotubes, leading to nonuniform emission energies in single nanotube measurements.[8,15,16]

The use of DNA for hybridization of carbon nanotube sidewalls has facilitated sorting nanotubes and building chemical sensors.[9,17−19] Single-strand DNA-wrapping introduces DNA segments with finite length, while the details of the secondary DNA structure will be determined by a complex interplay between $\pi-\pi$ stacking interactions between DNA bases and nanotube surface as well as electrostatic interactions of the phosphate backbone.[20−22] The effect of helical wrapping by the charged DNA backbone was modeled by applying a helical potential causing symmetry breaking of the nanotube electronic structure and small energetic shifts for semiconducting nanotubes (0.01 meV in water).[23,24] It is well-known that DNA-wrapping red-shifts the PL energy depending on the nanotube chirality by several tens of meV compared to the values reported for micelle-encapsulated nanotubes in aqueous solution,[7,25,26] which can be attributed to an increasing ε.[14] The surface coverage with DNA segments of finite length is expected to result in a nonuniform dielectric environment along the nanotubes.[25] Limited by diffraction, the PL information collected in confocal microscopy contains the optical response from a nanotube length of about 300 nm, which is far too large to clarify details of individual DNA−nanotube interactions. Tip-enhanced near-field optical microscopy (TENOM)[15,27,28] is ideally suited to visualize and quantify DNA-induced

* To whom correspondence should be addressed. E-mail: achim.hartschuh@cup.uni-muenchen.de.
[†] Ludwig-Maximilians-Universität München.
[‡] Universidade Federal de Minas Gerais.
[§] Northwestern University.
[||] University of Rochester.

10.1021/nl801038t CCC: $40.75
Published on Web 08/01/2008

modulations of the emission energy along single DNA−nanotube hybrid systems.

As a first step, we used confocal spectroscopy to study the PL from single DNA-wrapped and unwrapped nanotubes deposited on substrates. We found a strong red shift caused by DNA-wrapping of between 7 and 17 meV depending on the nanotube chirality. In the next step, TENOM was used to resolve PL variations along DNA-wrapped (6,5) and (6,4) nanotubes. Here two distinct emission bands are identified and assigned to emission from DNA-wrapped segments of the nanotube at E_{DNA} and unwrapped segments at E_0, distinguished by energy shifts of 18 meV for (6,5) and 30 meV for (6,4)- nanotubes, respectively. We were hereby able to spatially resolve the optical response of a nanotube to wrapping by a single DNA segment for the first time. Confocal emission spectra result from spatial averaging of the two peaks and show a peak at E_{conf} with a broadened spectral width of 40 meV. We further show that the transition between the two energetic levels occurs on a length scale smaller than our spatial resolution of 15 nm.

Our TENOM setup combines an inverted optical microscope with a sensitive shear-force feedback mechanism to position a sharp metal tip in the focus of the beam about 2 nm above the sample surface.[29] The samples studied are HiPCO nanotubes, DNA-wrapped HiPCO nanotubes spin-coated on glass, and (6,5) enriched DNA-wrapped CoMoCAT SWNTs spin-coated on a freshly cleaved thin mica layer glued on a glass cover slide. CoMoCAT SWNTs were sorted by using discriminating surfactants and wrapped by DNA after sorting. Density gradient ultracentrifugation isolates the narrow distributed, chirality enriched nanotubes.[17,30−32] The mica layer was positively charged with Mg^{2+} ions by exposure to 1 M $MgCl_2$ to make the negatively charged DNA site of the hybrid adhere to the surface.[20]

Figure 1 displays the histogram of PL emission energies from 203 HiPCO nanotubes (a), 235 DNA-wrapped HiPCO nanotubes spin-coated on glass (b), and 232 DNA-wrapped CoMoCAT nanotubes spin-coated on mica (c) obtained using confocal spectroscopy. The emission energies show a Gaussian distribution centered at energies that are assigned to different chiralities on the basis of literature data.[7] The emission energies of DNA-wrapped HiPCO nanotubes are red-shifted by 7−17 meV compared to unwrapped HiPCO nanotubes varying with nanotube chiralities as discussed in ref 25. DNA-wrapped CoMoCAT nanotubes on mica and DNA-wrapped HiPCO nanotubes on glass exhibit the same PL energies (Figure 1b and c) while the chirality distribution differs as a result of different catalytic growth and (6,5) enrichment in the case of the CoMoCAT material. In accordance with ref 25, DNA-wrapped (6,5) nanotubes show an emission energy of $E_{conf} = 1.249$ eV, whereas unwrapped (6,5) nanotubes emit at $E_0 = 1.256$ eV.

Figure 2 presents the near-field PL measurement of a DNA-wrapped CoMoCAT (6,5) SWNT spin-coated on mica. Figure 2a and b are the simultaneously recorded topography and near-field PL images, respectively. The scale bar indicates a lateral resolution of about 15 nm. The topographic height varies from 0.75 to 1.8 nm, indicating spatial

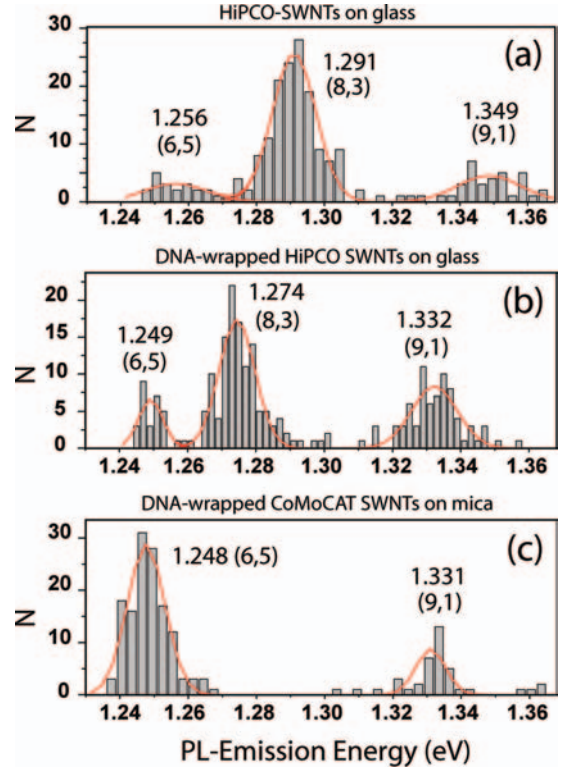

Figure 1. Histogram of PL emission energies from 203 HiPCO nanotubes (a), 235 DNA-wrapped HiPCO nanotubes spin-coated on glass (b), and 232 DNA-wrapped CoMoCAT nanotubes spin-coated on mica (c) upon laser excitation at 632.8 nm. The emission energies vary around center energies that are used for chirality assignment based on literature data.[7] DNA-wrapping causes a red shift for all chiralities. DNA-wrapped HiPCO and CoMoCAT nanotubes on different substrates have almost the same emission energies, while the histogram reflects the chirality distribution.

transitions between DNA-wrapped and unwrapped nanotube segments. While individual DNA segments forming a regular pitch are not resolved as in ref 20, the small height variation confirms the absence of large DNA aggregates and indicates nanotube wrapping by a single DNA layer. The PL image was obtained by measuring spectra at each pixel during the scan with an acquisition time of 0.4 s at a laser power of 100 μW. Figure 2b represents the integrated intensity from 970 to 1030 nm covering the emission range of (6,5) nanotubes.[7] First, the center emission energies were obtained by fitting the spectra with a single Lorentzian line shape function shown in Figure 2c and d. Apparently, the emission energy varies between 1.259 and 1.241 eV along the nanotube, as indicated by the two red dashed lines in Figure 2c, while the average of all near-field spectra at 1.249 eV coincides with the value from confocal far-field measurements. Figure 2d shows the variation of emission energy along the nanotube. Because the highest energy of 1.259 eV corresponds well to the value observed for unwrapped nanotubes of $E_0 = 1.256$ eV, we conclude that we detect parts of the nanotube that are not DNA-wrapped. In order to recover the average value observed in far-field measurements, DNA wrapping needs then to result in a larger red shift that can in fact be seen in the upper part of the nanotube with energies around 1.241 eV. Confocal measurements therefore

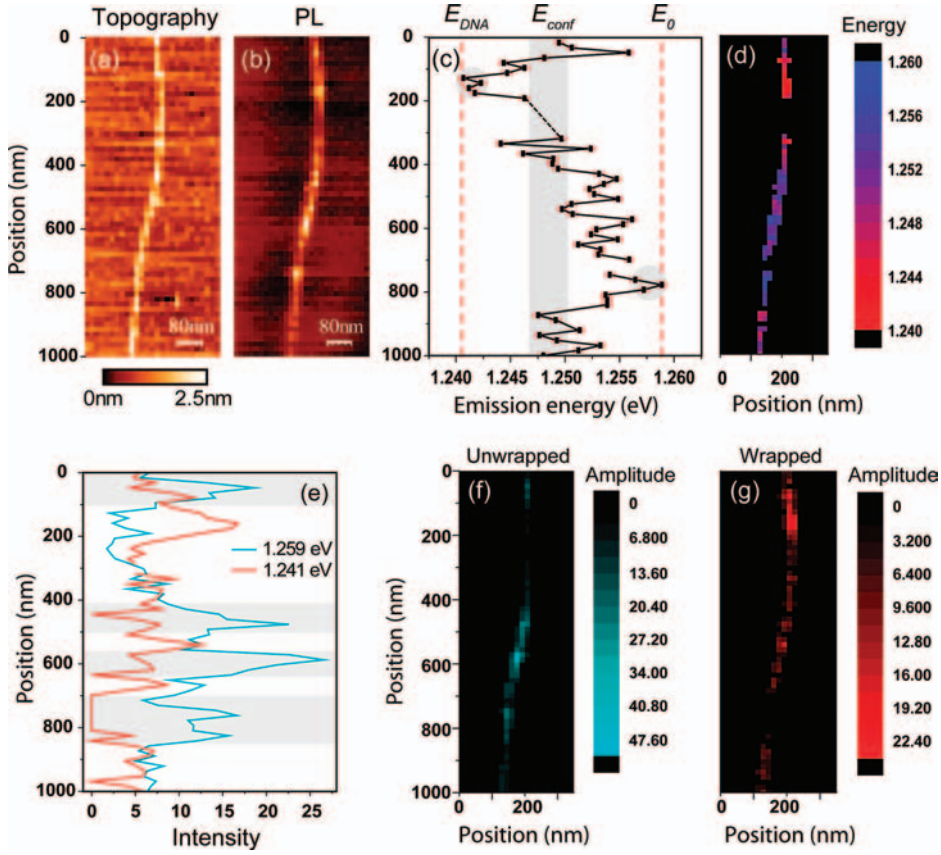

Figure 2. Simultaneously recorded topography (a) and near-field PL image (b) of a DNA-wrapped CoMoCAT (6,5) nanotube on mica. The PL image was obtained by measuring spectra at each pixel and represents the integrated intensity between 970 and 1030 nm covering the emission range of (6,5) nanotubes. For each pixel the emission spectrum was fitted with a single Lorentzian line shape function to extract the central emission energy that is plotted in (c) and (d). Strong energy variations occur between 1.259 and 1.241 eV on a length scale of about 20 nm (the error bar is about 0.7 meV indicated by the short red horizontal lines in (c)). The energy fluctuations occur around the confocal average $E_{conf} = 1.249$ eV that is marked by the vertical gray bar, while the maximum observed energy corresponds to the confocal average of unwrapped nanotubes $E_0 = 1.256$ eV marked by the dashed line. Apparently, some nanotube segments are not wrapped by DNA. (e−g) Fit results using two Lorentzian peak functions at E_0 and at E_{DNA}. The intensity profiles in (e) exhibit anticorrelation between the two peaks that can also be seen in the intensity images in (f) and (g).

underestimate the energy stabilization induced by DNA-wrapping by about a factor of 2. Similar near-field data obtained for (6,4) nanotubes indicates a DNA-induced energy shift of 30 meV (Figure 4c,f).

Limited by the spatial resolution of our experiment and the finite length of the DNA segments (~20 nm), the probed nanotube length will mostly contain both unwrapped and DNA-wrapped segments, leading to a superposition of emission bands at 1.259 and 1.241 eV, as can be seen in Figure 3e. When fitting the spectra with two Lorentzian peaks fixed at 1.259 and 1.241 eV representing unwrapped and wrapped sections, Figure 2b can be split into two PL images displaying the respective intensities of these sections (Figure 2f and g). The intensities of the two peaks show an anticorrelated behavior along the nanotube (Figure 2e−g) as expected for two distinct energetic levels. Figure 3 compares the confocal and near-field PL spectra of the (6,5) nanotube in Figure 2 obtained at position 150 and 750 nm as marked by gray circles in Figure 2c. Both confocal spectra (spectra a and b) show a single broad peak following a Gaussian line shape function with full width at half-maximum (fwhm) of 40 meV caused by the superposition of emission from both DNA-wrapped and unwrapped nanotube segments in the focus area. The near-field spectra resulting from a wrapped segment at 1.241 eV (spectrum c) and an unwrapped segment at 1.259 eV (spectrum d) are significantly sharper with fwhm of 27 and 25 meV, respectively. Spectrum e taken at a position ~80 nm on the other hand clearly shows two Lorentzian peaks (fwhm = 25 meV) at 1.240 and 1.259 meV, reflecting the simultaneous detection of emission from wrapped and unwrapped segments. In agreement with the energy distribution in Figure 2c, we mostly observe spectra containing two peaks. The near-field spectra detected here for DNA-wrapped (6,5) nanotubes are not only sharper than the confocal spectra of the material on substrates but are also found to be sharper than the conventional PL spectra of the material in solution of about 34 meV (data not shown).

Figure 4 illustrates the gradual transition between confocal far-field and near-field spectra upon approaching the tip at two different positions along a single (6,4) nanotube. The emission energies marked with white dashed lines in Figure 4a and d are from unwrapped and wrapped segments, respectively. For tip−sample distances larger than 20 nm, the detected signal represents the confocal spectrum resulting from spatial averaging. When the tip is closer within 10 nm

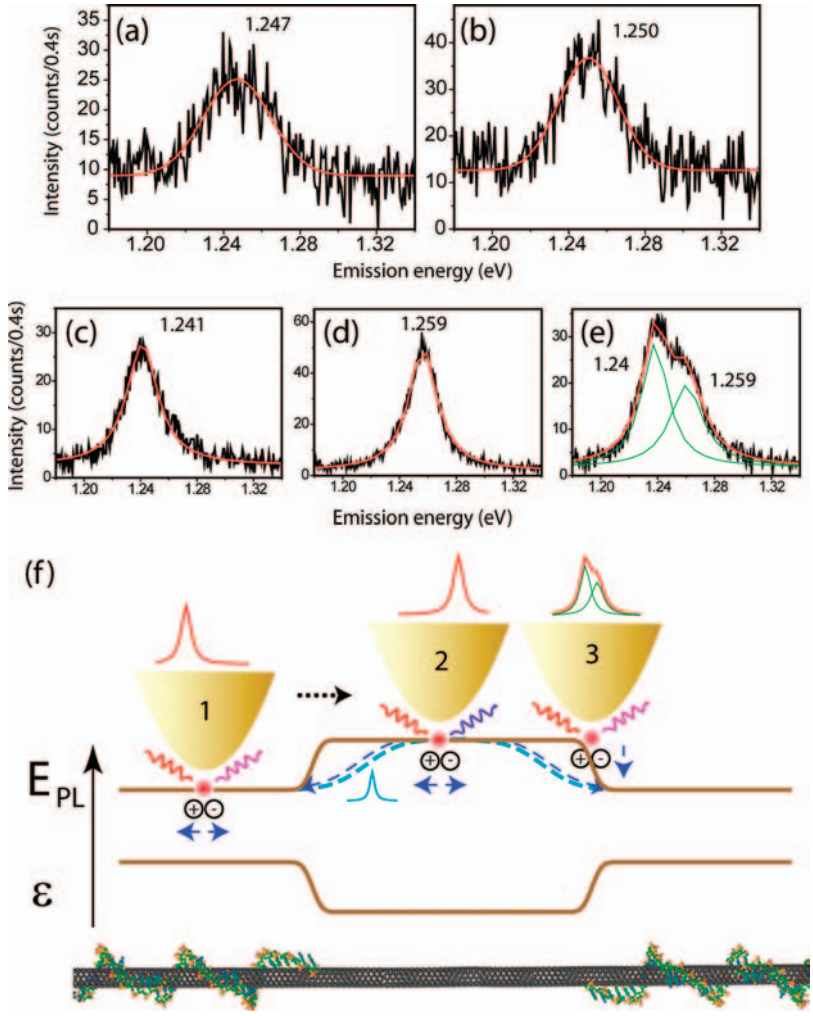

Figure 3. Confocal (a, b) and near-field (c−e) PL spectra of a DNA-wrapped CoMoCAT SWNT on mica together with Gaussian and Lorentzian fit curves for (a, b) and (c−e), respectively. Confocal and near-field spectra were detected at the locations along the nanotube in Figure 2c marked by gray circles. Both confocal spectra (a, b) feature a full width at half-maximum (fwhm) of 40 meV, while the near-field spectra (c, d) are significantly sharper with a fwhm of 27 and 25 meV, respectively. In the near-field spectrum (e) on the other hand two distinct peaks are clearly resolved with fwhm 25 meV attributed to DNA-wrapped and unwrapped sections of the nanotube. (f) Schematic illustration of the exited state energy E_{PL} landscape (brown line) along the DNA-wrapped nanotube including two wrapped parts with an unwrapped part in between, as indicated by the nanotube below. ε denotes the dielectric constant of the local environment reflecting local DNA wrapping. For the tip probing at different positions (numbers 1, 2, 3) on the nanotube, the expected spectra are shown on top of each position.

distance, a strong signal enhancement occurs (Figure 4b and e) and the near-field spectrum resulting from the nanotube section directly underneath the tip is detected. The peak energies during approaching observed for the two different positions along the nanotube are shown in Figure 4c and f and clearly resolve the transition between confocal and near-field dominated peak energies. Importantly, in the near-field regime within the last 5 nm, marked with red dashed lines in Figure 4, no spectral shift occurs within the precision of the measurement of about ±2 meV. Hence, the observed emission energy variations reported in our work are not affected by the presence of the metal tip and are caused only by DNA-wrapping.

In the following, we aim at extracting the transition length between red-shifted and non-shifted emissive states. To understand the origin of the different PL spectra, we illustrated the energy landscape and its modulation induced by the dielectric environment along the DNA-wrapped nanotube in Figure 3f schematically. The PL energy is lowered due to the increased dielectric constant ε associated with DNA-wrapping. Near-field scanning along the DNA-wrapped nanotube yields different optical responses when the tip is at different positions marked with numbers 1, 2 and 3. At position 1, the nanotube is locally excited on top of a DNA-wrapped segment and radiative exciton recombination occurs locally leading to low emission energy in the spectrum as shown in Figure 3c and indicated by the spectrum above the tip. At position 2 the tip probes the high emission energy of the bare nanotube as shown in Figure 3d. In the case of the tip probing on top of both DNA-wrapped and unwrapped parts depicted at position 3, the spectrum reveals double peaks including both low and high emission energies, as shown in Figure 3e. The simultaneous observation of two distinct emission peaks as in Figure 3e demonstrates that the transition between the two emissive energy levels occurs rapidly with respect to our spatial

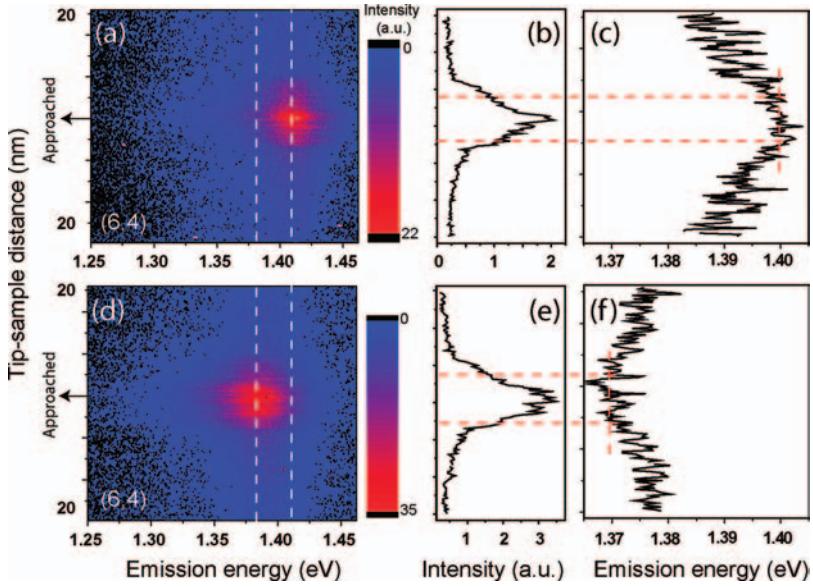

Figure 4. 2D photoluminescence maps taken at two different positions of a single (6,4) nanotube (a, d) as a function of tip−sample distance measured during tip approach and retracting. The difference between the two emission energies, marked by two white dashed lines, is due to DNA-wrapping. The PL intensity is strongly enhanced at small tip−sample distance and reaches the maximum when the tip is approached, marked by the arrows in (a) and (d), as shown in (b) and (e). The spectra are fit with single Lorentzian peak functions to determine the center emission energies at different tip−sample distances up to 20 nm and shown in (c) and (f) resolving the transition between confocal and near-field dominated peak energies. Within the near-field range, <5 nm guided by the red dashed line, the emission energies are constant within the experimental precision (±2 meV).

resolution, i.e., within less than 15 nm. In contrast, slower changes as indicated by the blue dashed line in Figure 3f would result in a single emission peak shifting in energy between high and low energy states.

Because nanotubes are extended one-dimensional systems, exciton mobility needs to be considered, increasing the complexity of the discussion. An exciton diffusional range of about 100 nm has been deduced from blinking traces.[33,34] In general, exciton mobility will result in an effective energy redistribution in which locally generated mobile excitons (blue arrows in Figure 3) would be trapped at lower energetic levels within a diffusional radius of about 100/2 nm = 50 nm. The ratio of emission intensities from the two states will therefore depend on the competition between exciton decay and exciton mobility, which is difficult to quantify experimentally. Moreover, the metal tip is expected to decrease the lifetime of the exciton by increasing both radiative and non-radiative decay rates,[15,35,36] which will reduce the effective exciton diffusional range and thereby increase the relative contribution of high energy emission. Remarkably, a single high energy peak is only observed at position 750 nm in Figure 2c−f, where the lower energy peak is absent for a long nanotube section of about 100 nm between 700−800 nm in agreement with this discussion.

Besides modifying the local dielectric environment of the nanotube, DNA−nanotube interactions could also result from charge transfer or local doping of the nanotube caused by the negatively charged DNA backbone. Charge carrier doping is predicted to reduce the PL intensity by phonon-assisted indirect exciton ionization,[37] and local quenching of PL was indeed observed for hole doping.[33] The nanotubes presented in Figure 2 and Figure 4 on the other hand showed extended and rather uniform emission intensities without signs of local quenching. We therefore have no indication for charge transfer involving the DNA backbone or the charged mica surface.

In summary, we present high resolution tip-enhanced near-field photoluminescence microscopy along DNA-wrapped CoMoCAT nanotubes. We resolve the PL energy shift along nanotubes induced by DNA segments, which turns out to be a factor of 2 higher than the value determined from confocal measurements representing spatial averaging. Based on the simultaneous detection of PL bands from both DNA-wrapped and unwrapped segments, we conclude that the transition between the two energetic levels occurs on a length scale smaller than our spatial resolution of 15 nm. Tip−sample distance dependent PL spectra confirm that the tip does not affect the emission energies within the near-field distance range. Our results demonstrate that nanotubes act as nanoscale reporters of their local dielectric environment, making them ideal candidates for sensing applications of single nanoobjects on a length scale of a few nanometers. Since wrapping by different DNA bases can be distinguished in ensemble measurements due to different PL energy shifts,[25] our results indicate that optical identification of single or few DNA bases can be achieved in the future.

Acknowledgment. The authors wish to acknowledge Steffen Schmidt (LMU) for SEM support. This work was funded by the Deutsche Forschungsgemeinschaft (DFG-HA4405/3-1 and the Nanosystems Initiative Munich (NIM)), the DAAD (Probral), and the U.S. Department of Energy (grant DE-FG02-05ER46207). Support from an Alfred P. Sloan Research Fellowship (M.C.H.) and a Natural Sciences and Engineering Research Council of Canada Fellowship (A.A.G.) are gratefully acknowledged. This work was also

funded by the U.S. National Science Foundation under Award Numbers EEC-0647560 and DMR-0706067. P.T.A. acknowledges CNPq and CAPES-Probral for financial support.

References

(1) *Carbon Nanotubes*; Jorio, A., Dresselhaus, M. S., Dresselhaus, G., Eds.; Springer: Berlin/Heidelberg, 2008; Vol. 111 of *Topics in Applied Physics*.
(2) Avouris, P.; Chen, J. *Mater. Today* **2006**, *9*, 46–54.
(3) Lu, W.; Lieber, C. M. *Nat. Mater.* **2007**, *6*, 841–850.
(4) Wang, F.; Dukovic, G.; Brus, L. E.; Heinz, T. F. *Science* **2005**, *308*, 838–841.
(5) Maultzsch, J.; Pomraenke, R.; Reich, S.; Chang, E.; Prezzi, D.; Ruini, A.; Molinari, E.; Strano, M. S.; Thomsen, C.; Lienau, C. *Phys. Rev. B* **2005**, *72*, 241402.
(6) Hagen, A.; Steiner, M.; Raschke, M. B.; Lienau, C.; Hertel, T.; Qian, H.; Meixner, A. J.; Hartschuh, A. *Phys. Rev. Lett.* **2005**, *95*, 197401.
(7) Bachilo, S. M.; Strano, M. S.; Kittrell, C.; Hauge, R. H.; Smalley, R.; Weisman, R. B. *Science* **2002**, *298*, 2361–2366.
(8) Hartschuh, A.; Pedrosa, H. N.; Novotny, L.; Krauss, T. D. *Science* **2003**, *301*, 1354–1356.
(9) Heller, D. A.; Jeng, E. S.; Yeung, T.-K.; Martinez, B. M.; Moll, A. E.; Gastala, J. B.; Strano, M. S. *Science* **2006**, *311*, 508–511.
(10) Perebeinos, V.; Tersoff, J.; Avouris, P. *Phys. Rev. Lett.* **2004**, *92*, 257402.
(11) Kiowski, O.; Lebedkin, S.; Hennrich, F.; Malik, S.; Rösner, H.; Arnold, K.; Sürgers, C.; Kappes, M. M. *Phys. Rev. B* **2007**, *75*, 075421.
(12) Ohno, Y.; Iwasaki, S.; Murakami, Y.; Kishimoto, S.; Maruyama, S.; Mizutani, T. *Phys. Rev. B.* **2006**, *73*, 235427.
(13) Walsh, A. G.; Vamivakas, A. N.; Yin, Y.; Cronin, S. B.; Ünlü, M. S.; Goldberg, B. B.; Swan, A. K. *Nano Lett.* **2007**, *7*, 1485–1488.
(14) Choi, J. H.; Strano, M. S. *Appl. Phys. Lett.* **2007**, *90*, 223114.
(15) Hartschuh, A.; Qian, H.; Meixner, A. J.; Anderson, N.; Novotny, L. *Nano Lett.* **2005**, *5*, 2310–2313.
(16) Htoon, H.; O'Connell, M. J.; Cox, P. J.; Doorn, S. K.; Klimov, V. I. *Phys. Rev. Lett.* **2004**, *93*, 027401.
(17) Zheng, M.; Jagota, A.; Semke, E. D.; Diner, B. A.; Mclean, R. S.; Lustig, S. R.; Richardson, R. E.; Tassi, N. G. *Nat. Mater.* **2003**, *2*, 338–342.
(18) Welsher, K.; Liu, Z.; Daranciang, D.; Dai, H. *Nano Lett.* **2008**, *8*, 586–590.
(19) Fantini, C. A.; Jorio, A.; Santos, A. P.; Peressinotto; V. S. T.; Pimenta, M. A. *Chem. Phys. Lett.* **2007**, *439*, 138–142.
(20) Jin, H.; Jeng, E. S.; Heller, D. A.; Jena, P. V.; Kirmse, R.; Langowski, J.; Strano, M. S. *Macromolecules* **2007**, *40*, 6731–6739.
(21) Johnson, R. R.; Charlie Johnson, A. T.; Klein, M. L. *Nano Lett.* **2008**, *8*, 69–75.
(22) Manohar, S.; Tang, T.; Jagota, A. *J. Phys. Chem. C* **2007**, *111*, 17835–17845.
(23) Michalski, P. J.; Mele, E. J. *Phys. Rev. B.* **2008**, *77*, 085429.
(24) Puller, V. I.; Rotkin, S. V. *Europhys. Lett.* **2007**, *77*, 27006.
(25) Jeng, E. S.; Moll, A. E.; Roy, A. C.; Gastala, J. B.; Strano, M. S. *Nano Lett.* **2006**, *6*, 371–375.
(26) Chou, S.; et al. *Chem. Phys. Lett.* **2004**, *397*, 296–301.
(27) *Tip Enhancement; Advances in Nano-Optics and Nano-Photonics*; Kawata, S., Shalaev, V. M., Eds.; Elsevier: Amsterdam, 2007.
(28) Qian, H.; Georgi, C.; Anderson, N.; Green, A. A.; Hersam, M. C.; Novotny, L.; Hartschuh, A. *Nano Lett.* **2008**, *8*, 1363–1367.
(29) Karrai, K.; Grober, R. D. *Appl. Phys. Lett.* **1995**, *66*, 1842–1844.
(30) Arnold, M. S.; Stupp, S. I.; Hersam, M. C. *Nano Lett.* **2005**, *5*, 713–718.
(31) Arnold, M. S.; Green, A. A.; Hulvat, J. F.; Stupp, S. I.; Hersam, M. C. *Nat. Nanotechnol.* **2006**, *1*, 60–65.
(32) Green, A. A.; Hersam, M. C. *Mater. Today* **2007**, *10*, 59–60.
(33) Cognet, L.; Tsyboulski, D. A.; Rocha, J. D. R.; Doyle, C. D.; Tour, J. M.; Weisman, R. B. *Science* **2007**, *316*, 1465–1468.
(34) Georgi, C.; Hartmann, N.; Gokus, T.; Green, A. A.; Hersam, M. C.; Hartschuh, A. *Chem. Phys. Chem.* **2008**, *9*, 1460.
(35) Anger, P.; Bharadwaj, P.; Novotny, L. *Phys. Rev. Lett.* **2006**, *96*, 113002.
(36) Kühn, S.; Hakanson, U.; Rogobete, L.; Sandoghdar, V. *Phys. Rev. Lett.* **2006**, *96*, 017402.
(37) Perebeinos, V.; Avouris, P. cond. Mat. arXiv:0804.0767v2, **2008**.

NL801038T